

Charge Asymmetry Suppresses Coarsening Dynamics in Polyelectrolyte Complex Coacervation

Shensheng Chen¹ and Zhen-Gang Wang^{1*}

Division of Chemistry and Chemical Engineering, California Institute of Technology, Pasadena, California 91125, USA

 (Received 24 August 2023; accepted 2 November 2023; published 21 November 2023)

Mixing solutions of oppositely charged macromolecules can result in liquid-liquid phase separation into a polymer-rich coacervate phase and a polymer-poor supernatant phase. Here, we show that charge asymmetry in the constituent polymers can slow down the coarsening dynamics, with an apparent growth exponent that deviates from the well-known $1/3$ for neutral systems and decreases with increasing degrees of charge asymmetry. Decreasing solvent quality accelerates the coarsening dynamics for asymmetric mixtures but slows down the coarsening dynamics for symmetric mixtures. We rationalize these results by examining the interaction potential between merging droplets.

DOI: [10.1103/PhysRevLett.131.218201](https://doi.org/10.1103/PhysRevLett.131.218201)

The association of macromolecules in solution often results in liquid-liquid phase separation (LLPS), with the formation of a polymer-rich liquid phase (coacervate) coexisting with a dilute (supernatant) phase. The liquidlike coacervates, which can be formed by complexation of oppositely charged polyelectrolytes (PEs) and/or by protein association, are of great importance in materials and biology [1,2]. The formation of these liquid coacervates involves the coarsening of small droplets into larger droplets [1,3,4]. For biocondensates and PE complex coacervates, the coarsening process is experimentally found to be significantly slower than the theoretically anticipated spinodal decomposition dynamics for solutions of uncharged polymers, for which the evolution of domain coarsening follows the well-known power law $R \sim t^\beta$ with $\beta = 1/3$ [5]. For example, Lee, Wingreen, and Brangwynne [3] found the coarsening dynamics in LLPS of biocondensates in the cellular environment is considerably suppressed, with a growth exponent $\beta \approx 0.12$. The coarsening in biocondensate coacervate usually stops with multiple stable droplets [3,6–8]. Liu *et al.* [9,10] found that the coarsening dynamics is also suppressed in LLPS of PE complex coacervation from mixing oppositely charged PE solutions, with $\beta = 0.093$ – 0.18 .

The suppressed coarsening dynamics in coacervate formation suggests that the merging of small droplets does not follow the downward free energy path (constrained by material diffusion) as in the classical spinodal decomposition mechanism. Possible explanations to the origin of the suppressed dynamics in the LLPS in biocondensate coacervates include the coupling of the phase separation to the elastic deformation of an underlying chromatin network [3,7,11] or nonequilibrium activities in the cellular environments [12,13]. While these mechanisms are reasonable for LLPS dynamics in biocondensates in the cells, they cannot explain the observed deviations from simple spinodal decomposition dynamics in PE complex

coacervation. A common feature in both biocondensate coacervates and PE complex coacervates is that these coacervate droplets involve charged macromolecules. The macromolecular charges in the droplets are, in general, not balanced [14–17]—perfect charge balance is the exception rather than the rule. The charge asymmetry between polycations and polyanions (or, in the case of biocondensates, the unequal number of positively and negatively charged residues on the biomacromolecules), in general, gives rise to net-charged clusters carrying the sign of the overall net charge of the macromolecules [17]. The interaction between charged droplets is expected to create a free energy barrier that can potentially slow down the coarsening dynamics and, in the case of highly asymmetric systems, even stop the coarsening process, resulting in finite-sized clusters [17–21].

In this Letter, we examine the effects of charge asymmetry on the dynamics of LLPS by simulating the coarsening of PE coacervate droplets under different charge asymmetry and solvent quality conditions using electrostatic dissipative particle dynamics (EDPD) simulation [17,22,23]. In our DPD simulation, monomers of polycations and polyanions, their counterions, and solvent (water) are explicitly modeled by coarse-grained beads having the same mass m and size r_c . Nonbonded beads interact with each other via a soft repulsive force given by $F_{ij}^C = a_{ij}(1 - r_{ij}/r_c)\mathbf{e}_{ij}$, where a_{ij} is the strength of the interaction, $r_{ij} = |\mathbf{r}_i - \mathbf{r}_j|$ is the interbead distance, and $\mathbf{e}_{ij} = (\mathbf{r}_i - \mathbf{r}_j)/r_{ij}$ represents the direction of the force. We set the repulsion a_{ij} between all species as $a_{ij} = 75k_B T/r_c$, with the exception of repulsion between the monomer on the polyion and water a_{pw} , whose value is given by $a_{pw} = 75k_B T/r_c + \Delta a$ to control the solvent condition by adjusting Δa . Here, $k_B T$ is the thermal energy, and we take T to be the room temperature. $\Delta a \leq 0$ corresponds to good

solvent, and increasing Δa decreases the solvent quality. Although it is possible to map the values of Δa to the more familiar Flory-Huggins parameter, such a mapping is more appropriate for neutral systems and requires fitting to a particular model. Here, we will simply report the value of Δa . The thermostat in DPD is controlled by two additional pairwise forces, the dissipative force and the random force, which are related by the fluctuation-dissipation theorem, with the force parameters given by Groot and Warren [24]. Since all the forces in the DPD are pairwise, momentum conservation is guaranteed, allowing hydrodynamics to be captured at the mesoscale.

The polymers are modeled as beads connected by a harmonic bond potential $E_{\text{bond}} = \frac{1}{2}K_{\text{bond}}(r - r_0)^2$ between two consecutive beads along linear chains. The bond strength and equilibrium bond length are set to $K_{\text{bond}} = 100k_B T/r_c^2$ and $r_0 = 0.5r_c$, respectively. m , $k_B T$, and r_c represent the mass, energy, and length units, respectively, in DPD simulations, which are all set to unity. With the typical interpretation that one DPD bead corresponds to three water molecules [22,24], r_c has a physical length of 0.64 nm. Each monomer in polycations (polyanions) carries unit charge of $+e$ ($-e$), and the corresponding counterion has the opposite unit charge. The Bjerrum length is set to $l_B = 0.7$ nm to represent the electrostatic interaction strength in water at room temperature. Electrostatic interactions are calculated by solving the Poisson equation in real space in the simulation domain, in which the electric field is computed on a mesh with smeared charges from the off-lattice point charges, as detailed in Ref. [22]. The total monomer concentration is about 0.14 M. Together with the counterions, the total ion concentration (cation and anion) is 0.28 M, corresponding to a nominal Debye screening length of about 1 nm. Other simulation details are given in Supplemental Material [25].

Our simulations include 125 fully charged polycations with chain length N_1 and 125 polyanions with chain length N_2 in a box of $60 \times 60 \times 60 r_c^3$. The elementary process of polyelectrolyte complex coacervation consists of the formation of polycation-polyanion pairs followed by the coalescence of the pairs into larger clusters [4,26]. Since the experiments monitored only the coarsening process, the initial states right after the mixing of the polycation and polyanion solutions are unknown. We, thus, initialize our system by having 125 small droplets each consisting of a polycation-polyanion pair. Similar to the experimental measurements [3,7], we monitor the coarsening dynamics by calculating the time evolution of the (number) average radius of gyration $\langle R \rangle$ of the clusters in the system. The degree of charge asymmetry is defined by $\lambda = N_1/N_2$, where for concreteness we take $N_1 \leq N_2$ and keep $N_1 + N_2 = 80$. For each charge asymmetry, we perform ten independent runs to obtain the ensemble average. During each individual simulation, we observe that the average droplet size in the system increases in a discrete

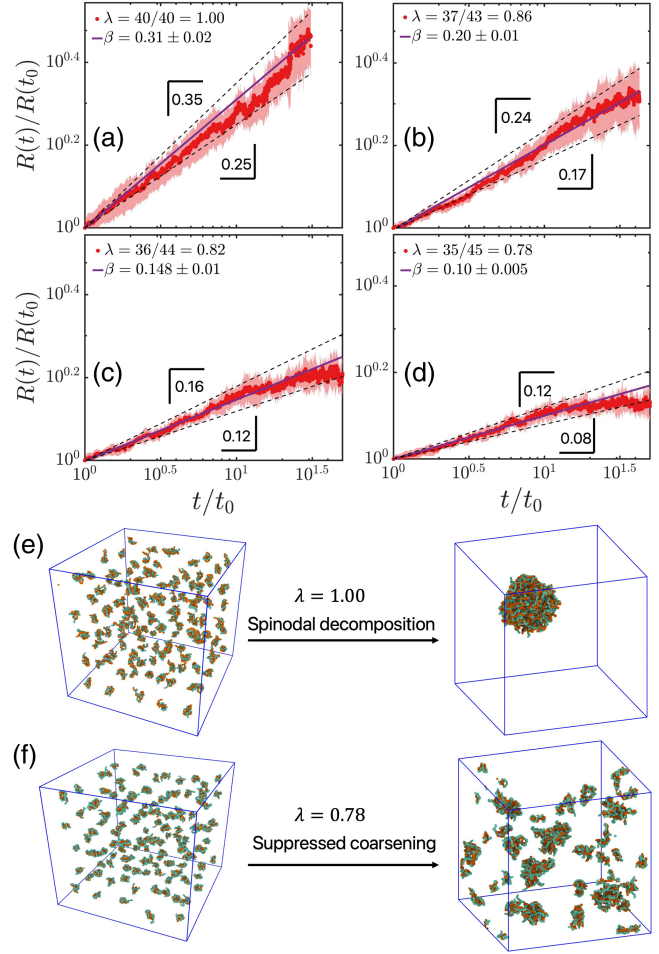


FIG. 1. (a)–(d) Domain growth in systems with charge ratio (between polycation and polyanion) $\lambda = 1.00, 0.86, 0.82, 0.78$. The solid lines show the best-fitted scaling exponents, while the dashed lines are the upper and lower bounds of the exponents. $t_0 = 400, 165, 125, \text{ and } 100$ in DPD time, from (a) to (d), respectively. The shaded areas represent standard deviation from ten independent runs. (e), (f) Simulation snapshots before and after domain coarsening for $\lambda = 1.00$ and $\lambda = 0.78$, respectively. The green and orange beads represent polycation and polyanion monomers, respectively. Solvent molecules and counterions are not shown for clarity.

“stepwise” fashion, and the small droplets maintain their composition before merging into larger droplets. These observations indicate that the domain growth is driven by droplet coarsening, instead of Ostwald ripening; the same conclusion was reached in the experimental studies of coarsening dynamics in biocondensates [3,7].

We first consider the effects of charge asymmetry λ under good solvent condition ($\Delta a = 0$). Figures 1(a)–1(d) show the time evolution of $R(t)/R(t_0)$ for different values of λ , where $R(t_0)$ is the average radius of gyration in the systems at time t_0 when the size first shows power-law growth. For the charge-balanced system ($\lambda = 1$), Fig. 1(a) shows the coarsening dynamics follows a power-law scaling $\sim t^{0.31}$,

which is very close to the theoretically expected $1/3$ scaling for spinodal decomposition. The slight deviation from $1/3$ is likely due to the finite-size effect in simulations (since there are very few droplets in the later stages of the simulation). In all the runs for the charge-balanced systems, the coarsening ends up with the formation of a single large droplet containing all the polyions, as shown in Fig. 1(e). With charge asymmetry, the phase separation dynamics slows down significantly: The apparent power law $\sim t^\beta$ in domain growth has a smaller exponent of $\beta = 0.20, 0.14,$ and 0.10 , respectively, for $\lambda = 0.86, 0.82, 0.78$. These values are quite close to the range of the exponents observed in the experiments [3,9]. For $\lambda = 0.82$ and 0.78 , the coarsening stops with multiple droplets carrying net negative charges as the final state; a snapshot is shown in Fig. 1(f). This result is consistent with experimental observation and with our recent finding on the equilibrium behavior in the complex coacervation of charge-asymmetric polyelectrolyte mixtures [16,17]. For the case of $\lambda = 0.86$, the final state consists of 3–5 clusters; On the other hand, if we artificially put all the polymers into a single droplet, the droplet remains stable without spontaneous fission, as shown in Fig. S1 in Supplemental Material [25]. For $\lambda = 0.78$ and $\lambda = 0.82$, the artificially created single droplet splits into multiple smaller droplets, suggesting that the equilibrium state contains multiple droplets at these conditions. Whether the final state obtained in our coarsening simulation represents the equilibrium state or a metastable state due to kinetic barriers for fusion remains to be investigated further.

To understand the observed slowdown in the coarsening dynamics due to charge asymmetry, we examine the elementary process of the merging of two polyion pairs into a two-pair cluster. To this end, we compute the potential of mean force (PMF) between the two polyion pairs as a function of their center-of-mass distance r [27–29]; the result is shown in Fig. 2, for the case of good solvent condition ($\Delta a = 0$) under different charge ratios.

For the symmetric system ($\lambda = 1$), the coalescence of the two droplets experiences no free energy barrier, consistent with the spinodal decomposition mechanism. For all three cases with charge asymmetry, coalescence of the two droplets involves an energy barrier along the pathway, with the barrier height increasing with increasing charge asymmetry (i.e., decreasing λ), consistent with the slower coarsening dynamics for the more charge-asymmetric systems. Clearly, the free energy barrier must arise from the repulsion between droplets carrying net macromolecular charges. Note that the free energy barriers are of the order of $k_B T$ or less; thus, thermal fluctuation can easily drive the fusion of these polyion pairs. As the droplets grow and accumulate more net charge, we expect the free energy barrier for coalescence to increase, which can eventually arrest further growth. Note that macromolecular condensates carrying net charges can have preferred size as the

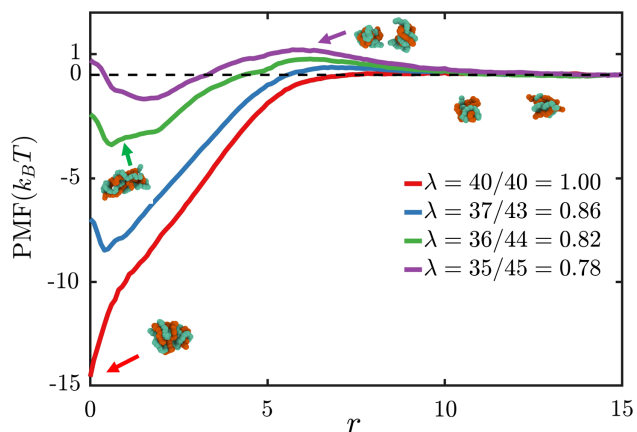


FIG. 2. Potential of mean force for complexation of two polyion pairs under different charge ratios $\lambda = 1.00, 0.86, 0.82, 0.78$ in good solvent condition.

final equilibrium state or as an intermediate metastable state [30]. So the final state observed in our simulation for these asymmetric systems can be due to both thermodynamic and kinetic reasons.

Theoretically, droplet coalescence and coarsening are driven by the tendency to decrease the surface energy. Therefore, we expect that coarsening dynamics should be faster with decreasing solvent quality [5]. To this end, we study the LLPS dynamics in systems with charge ratio $\lambda = 0.78$ under different solvent conditions with $\Delta a = 0, 10, 25$. Figure 3 shows the coarsening dynamics is indeed accelerated—as evidenced by larger droplet sizes and larger apparent power-law exponent—with increasing Δa . In addition, coarsening proceeds further, since the final state contains fewer and larger droplets. However, even for $\Delta a = 25$, which corresponds to a very poor solvent, the growth exponent reaches about $\beta = 0.2$, significantly below the $\sim 1/3$ observed in charge-balanced systems. These results suggest that, while poor solvent conditions

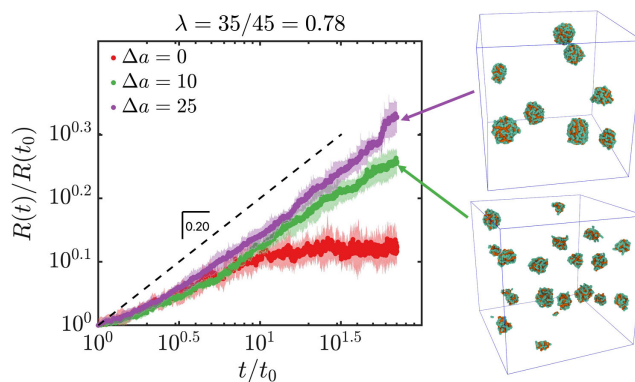


FIG. 3. Domain growth in systems with charge ratio $\lambda = 0.78$ for solvent conditions at $\Delta a = 0, 10, 25$, respectively. The simulation snapshots on the right shows the final morphology of the systems containing multiple net-charged droplets.

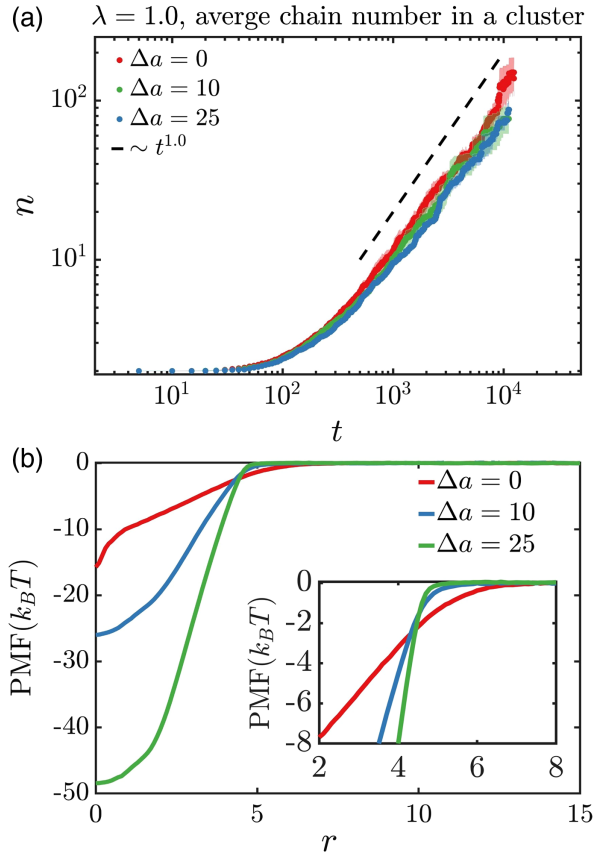


FIG. 4. (a) Time evolution of chain number in a cluster in charge-balanced systems under solvent conditions of $\Delta a = 0, 10, 25$. The coarsening dynamics, in general, follow the theoretical $1/3$ domain growth law. With increasing Δa , the domain growth is slightly slower. (b) PMF profile for complexation of two charge-balance pairs under solvent condition of charge asymmetry of $\Delta a = 0, 10, 25$. Although larger Δa gives deeper attractive wells, smaller Δa has larger distance to trigger the attraction between the droplets, which can be seen more clearly in the inset.

can accelerate the coarsening dynamics, electrostatic repulsion between droplets in asymmetric systems still has strong effects in suppressing the coarsening dynamics and preventing the complete coalescence of all the droplets.

The effects of solvent condition on LLPS dynamics in the charge-balanced systems are shown in Fig. 4(a), where we plot the time evolution of the average number of chains n in a cluster. Not surprisingly, the coarsening dynamics in all three solvent conditions approximately follow the $t^{1/3}$ domain growth law (noting that $n \sim R^3 \sim t^{3\beta}$), consistent with the barrierless process for spinodal decomposition; see Fig. 4(b). Surprisingly, however, decreasing the solvent quality results in a slight but clearly noticeable slowdown of the coarsening dynamics. This is quite different from the expected behavior for LLPS in neutral systems, where decreasing the solvent quality generally results in faster coarsening dynamics [5]. A possible reason is that the

attraction due to mutual polarization between two approaching polyion globules is slightly stronger in good solvent than in poor solvent due to the smaller surface tension and lower polymer density in the former, as shown in Figs. 4(b) and S2 in Supplemental Material [25]. In addition, the smaller surface tension and lower polymer density make the droplets more susceptible to shape fluctuation, thus facilitating contacts that trigger the coalescence.

In summary, we have shown that the charge asymmetry significantly suppresses the coarsening dynamics in polyelectrolyte complex coacervation. Decreasing the solvent quality can accelerate coarsening in charge-asymmetric systems but cannot recover the $t^{1/3}$ growth law for the classical spinodal decomposition. For the charge-balanced system, however, decreasing the solvent quality slows down the coarsening dynamics while still maintaining the $t^{1/3}$ power law growth. While these results are obtained for LLPS dynamics in an idealized model of polyelectrolyte complex coacervation, our results are consistent with the experimental observations by Liu *et al.* [9,10] for complex coacervation in synthetic polyelectrolytes. In addition, a recent experimental study of biocondensates formed by peptide and RNA complexation with unbalanced charges shows that nearly all the droplets formed carry the same sign of charges [31], consistent with our simulation setup. We, thus, expect our findings to be relevant to biocondensates involving biomacromolecules that are not charge balanced. To capture the behaviors in specific systems, more realistic features, such as chain structure and charge polydispersity, as well as the presence of other charged species, need to be taken into account. More studies are warranted to explore the effects of electrostatics in LLPS in cells and in biomimetic systems.

This research is supported by funding from Hong Kong Quantum AI Lab, AIR@InnoHK of Hong Kong Government. This research used resources of the Center for Functional Nanomaterials (CFN), which is a U.S. Department of Energy Office of Science User Facility, at Brookhaven National Laboratory under Contract No. DE-SC0012704. We thank Dr. Andrew Ylitalo for useful discussions.

*zgw@caltech.edu

- [1] S. F. Banani, H. O. Lee, A. A. Hyman, and M. K. Rosen, Biomolecular condensates: Organizers of cellular biochemistry, *Nat. Rev. Mol. Cell Biol.* **18**, 285 (2017).
- [2] Y. Shin and C. P. Brangwynne, Liquid phase condensation in cell physiology and disease, *Science* **357**, aaf4382 (2017).
- [3] D. S. W. Lee, N. S. Wingreen, and C. P. Brangwynne, Chromatin mechanics dictates subdiffusion and coarsening dynamics of embedded condensates, *Nat. Phys.* **17**, 531 (2021).

- [4] S. Chen and Z.-G. Wang, Driving force and pathway in polyelectrolyte complex coacervation, *Proc. Natl. Acad. Sci. U.S.A.* **119**, e2209975119 (2022).
- [5] E. D. Siggia, Late stages of spinodal decomposition in binary mixtures, *Phys. Rev. A* **20**, 595 (1979).
- [6] Y. Shin, Y.-C. Chang, D. S. W. Lee, J. Berry, D. W. Sanders, P. Ronceray, N. S. Wingreen, M. Haataja, and C. P. Brangwynne, Liquid nuclear condensates mechanically sense and restructure the genome, *Cell* **175**, 1481 (2018).
- [7] Y. Zhang, D. S. Lee, Y. Meir, C. P. Brangwynne, and N. S. Wingreen, Mechanical frustration of phase separation in the cell nucleus by chromatin, *Phys. Rev. Lett.* **126**, 258102 (2021).
- [8] J. Berry, C. P. Brangwynne, and M. Haataja, Physical principles of intracellular organization via active and passive phase transitions, *Rep. Prog. Phys.* **81**, 046601 (2018).
- [9] X. Liu, M. Haddou, I. Grillo, Z. Mana, J.-P. Chapel, and C. Schatz, Early stage kinetics of polyelectrolyte complex coacervation monitored through stopped-flow light scattering, *Soft Matter* **12**, 9030 (2016).
- [10] X. Liu, J.-P. Chapel, and C. Schatz, Structure, thermodynamic and kinetic signatures of a synthetic polyelectrolyte coacervating system, *Adv. Colloid Interface Sci.* **239**, 178 (2017).
- [11] Y. Qi and B. Zhang, Chromatin network retards nucleoli coalescence, *Nat. Commun.* **12**, 6824 (2021).
- [12] H. Falahati and E. Wieschaus, Independent active and thermodynamic processes govern the nucleolus assembly *in vivo*, *Proc. Natl. Acad. Sci. U.S.A.* **114**, 1335 (2017).
- [13] J. D. Wurtz and C. F. Lee, Chemical-reaction-controlled phase separated drops: Formation, size selection, and coarsening, *Phys. Rev. Lett.* **120**, 078102 (2018).
- [14] C. Pak, M. Kosno, A. Holehouse, S. Padrick, A. Mittal, R. Ali, A. Yunus, D. Liu, R. Pappu, and M. Rosen, Sequence determinants of intracellular phase separation by complex coacervation of a disordered protein, *Mol. Cell* **63**, 72 (2016).
- [15] Y. Yin, L. Niu, X. Zhu, M. Zhao, Z. Zhang, S. Mann, and D. Liang, Non-equilibrium behaviour in coacervate-based protocells under electric-field-induced excitation, *Nat. Commun.* **7**, 10658 (2016).
- [16] A. Agrawal, J. F. Douglas, M. Tirrell, and A. Karim, Manipulation of coacervate droplets with an electric field, *Proc. Natl. Acad. Sci. U.S.A.* **119**, e2203483119 (2022).
- [17] S. Chen, P. Zhang, and Z.-G. Wang, Complexation between oppositely charged polyelectrolytes in dilute solution: Effects of charge asymmetry, *Macromolecules* **55**, 3898 (2022).
- [18] R. Zhang and B. Shklovskii, Phase diagram of solution of oppositely charged polyelectrolytes, *Physica (Amsterdam)* **352A**, 216 (2005).
- [19] T. T. Nguyen and B. I. Shklovskii, Kinetics of macroion coagulation induced by multivalent counterions, *Phys. Rev. E* **65**, 031409 (2002).
- [20] N. N. Oskolkov and I. I. Potemkin, Complexation in asymmetric solutions of oppositely charged polyelectrolytes: Phase diagram, *Macromolecules* **40**, 8423 (2007).
- [21] A. M. Romyantsev and I. I. Potemkin, Explicit description of complexation between oppositely charged polyelectrolytes as an advantage of the random phase approximation over the scaling approach, *Phys. Chem. Chem. Phys.* **19**, 27580 (2017).
- [22] R. D. Groot, Electrostatic interactions in dissipative particle dynamics—simulation of polyelectrolytes and anionic surfactants, *J. Chem. Phys.* **118**, 11265 (2003).
- [23] S. Plimpton, Fast parallel algorithms for short-range molecular dynamics, *J. Comput. Phys.* **117**, 1 (1995).
- [24] R. D. Groot and P. B. Warren, Dissipative particle dynamics: Bridging the gap between atomistic and mesoscopic simulation, *J. Chem. Phys.* **107**, 4423 (1997).
- [25] See Supplemental Material at <http://link.aps.org/supplemental/10.1103/PhysRevLett.131.218201> for additional details on DPD simulation, calculation of PMF, discussion of the stability of a charge-asymmetric droplet, and mutual polarization between two charged-balanced droplets.
- [26] K. T. Delaney and G. H. Fredrickson, Theory of polyelectrolyte complexation—Complex coacervates are self-coacervates, *J. Chem. Phys.* **146**, 224902 (2017).
- [27] E. Darve, D. Rodríguez-Gómez, and A. Pohorille, Adaptive biasing force method for scalar and vector free energy calculations, *J. Chem. Phys.* **128**, 144120 (2008).
- [28] J. Comer, J. C. Gumbart, J. Hémin, T. Lelièvre, A. Pohorille, and C. Chipot, The adaptive biasing force method: Everything you always wanted to know but were afraid to ask, *J. Phys. Chem. B* **119**, 1129 (2015).
- [29] G. Fiorin, M. L. Klein, and J. Hémin, Using collective variables to drive molecular dynamics simulations, *Mol. Phys.* **111**, 3345 (2013).
- [30] S. B. Hutchens and Z.-G. Wang, Metastable cluster intermediates in the condensation of charged macromolecule solutions, *J. Chem. Phys.* **127**, 084912 (2007).
- [31] T. J. Welsh, G. Krainer, J. R. Espinosa, J. A. Joseph, A. Sridhar, M. Jahnelt, W. E. Arter, K. L. Saar, S. Alberti, R. Collepardo-Guevara, and T. P. J. Knowles, Surface electrostatics govern the emulsion stability of biomolecular condensates, *Nano Lett.* **22**, 612 (2022).